Ricin–Membrane Interaction: Membrane Penetration Depth by Fluorescence Quenching and Resonance Energy Transfer†

T. S. Ramalingam,‡ Puspendu Kumar Das,*,‡ and Sunil K. Podder*,§

Department of Inorganic and Physical Chemistry and Department of Biochemistry, Indian Institute of Science, Bangalore 560012, India

Received January 24, 1994; Revised Manuscript Received April 26, 1994®

ABSTRACT: The entry of the plant toxin ricin and its A- and B-subunits in model membranes in the presence as well as absence of monosialoganglioside (GM_1) has been studied. Dioleoylphosphatidylcholine and 5-, 10-, and 12-doxyl- or 9,10-dibromophosphatidylcholines serve as quenchers of intrinsic tryptophan fluorescence of the proteins. The parallax method of Chattopadhyay and London [(1987) *Biochemistry 26*, 39–45] has been employed to measure the average membrane penetration depth of tryptophans of ricin and its B-chain and the actual depth of the sole Trp 211 in the A-chain. The results indicate that both of the chains as well as intact ricin penetrate the membrane deeply and the C-terminal end of the A-chain is well inside the bilayer, especially at pH 4.5. An extrinsic probe *N*-(iodoacetyl)-*N'*-(5-sulfo-1-naphthyl)ethylenediamine (I-AEDANS) has been attached to Cys 259 of the A-chain, and the kinetics of penetration has been followed by monitoring the increase in AEDANS fluorescence at 480 nm. The insertion follows first-order kinetics, and the rate constant is higher at a lower pH. The energy transfer distance analysis between Trp 211 and AEDANS points out that the conformation of the A-chain changes as it inserts into the membrane. CD studies indicate that the helicity of the proteins increases after penetration, which implies that some of the unordered structure in the native protein is converted to the ordered form during this process. Hydrophobic forces seem to be responsible for stabilizing a particular protein conformation inside the membrane.

Toxins of both bacterial and plant origins have a common ability to inhibit protein synthesis in eukaryotic cells (Olsnes & Pihl, 1980; Gill et al., 1981). Most of them consist of two chains. One binds carbohydrate(s), and the other exerts the toxic activity by blocking protein synthesis. To exercise lethal activity, both plant and bacterial toxins have to translocate across the hydrophobic membrane barrier (Sekharam et al., 1991). Ricin, a plant toxin, is made up of two polypeptide chains, A and B, connected by a disulfide bond. This toxin assumes importance because of its potential application in immunotoxin preparation (Blatter et al., 1989; Vietta & Thorpe, 1993). To devise an immunotoxin with defined specificity, it is essential to know the mechanism of its action. From studies on cells it is known that the cleavage of the disulfide bond connecting the A and B chains is necessary for this toxin to exercise its toxicity (Montessaro et al., 1982). It is also believed that acidic compartments such as late endosomes are probable sites for the transmembrane transfer of intact ricin into the cytosol (Beaumelle et al., 1993; Frenoy et al., 1992) where the A-chain is liberated. This A-chain, in turn, goes to the ribosomal RNA and stops protein synthesis.

Ricin is highly water soluble and is known to interact with model membranes in the presence as well as absence of GM_1[1] (Utsumi et al., 1984, 1987). The *in vivo* studies with immunotoxins point out a dual role of the B-chain. In addition to binding to the membrane surface, it helps the entry of the intact toxin into the cytosol. Until recently it was believed that only the A-chain is capable of translocating itself (Houston, 1982), but it has been pointed out *in vivo* that both the A- and B-chains display translocation ability (Calafat et al., 1988; Beaumelle et al., 1993). During this process they must interact with phospholipid bilayers to reach the intracellular target. Though much is known about the diphtheria toxin interaction with the membrane (London, 1992), very little is, in fact,, known about ricin membrane interaction. Diphtheria toxin at low pH ($\sim$5) encountered at the endosome undergoes conformational changes resulting in a selective transfer of the A-chain through the endosomal membrane (Beaumelle et al., 1992; Olsnes & Pihl, 1988; Donovan et al., 1985). Direct insertion of A and B fragments of diphtheria toxin in model membranes has also been reported (Hu & Holmes, 1984). Here we address the interaction of the A- and B-chains of ricin as well as the intact protein with the membrane. The kinetics of free A-chain penetration into model membranes has also been probed.

Fluorophore quenching by spin labels sitting inside a lipid bilayer (Chattopadhyay & London, 1987; Abrams et al., 1992) has been employed to determine the depth of acetylcholine receptor from *Torpedo californica* in reconstituted membranes (Chattopadhyay & McNamee, 1991) and of membrane-inserted diphtheria toxin (Jiang et al., 1991). The measured average depths of tryptophan were 10.1 Å in nicotinic acetylcholine receptor and 8.3 Å in diphtheria toxin. In our work, fluorescence of the intrinsic tryptophan moieties of the protein is quenched by either doxyl spin labels or bromine atoms attached covalently to the fatty acyl chains (Markello et al., 1985) of the lipids forming vesicles. While the exact location of the sole tryptophan, Trp 211, of the A-chain in the bilayer has been determined, for ricin and its B-chain only an average depth could be estimated. The insertion kinetics using

† S.K.P. thanks CSIR, Government of India, for partly funding this research.

‡ Department of Inorganic and Physical Chemistry.

§ Department of Biochemistry.

® Abstract published in *Advance ACS Abstracts,* June 15, 1994.

[1] Abbreviations: GM_1, monosialoganglioside; DOPC, dioleoyl-*sn*-glycero-3-phosphatidylcholine; EDTA, ethylenediaminetetraacetic acid; HEPES, *N*-(2-hydroxyethyl)piperizine-*N'*-(2-ethanesulfonic acid); I-AEDANS, *N*-(iodoacetyl)-*N'*-(5-sulfo-1-naphthyl)ethylenediamine; ESR, electron spin resonance; CD, circular dichroism; TEMPO, 2,2,6,6-tetramethylpiperidine-1-oxyl; DTT, dithiothreitol; UV, ultraviolet; SDS–PAGE, sodium dodecyl sulfate–polyacrylamide gel electrophoresis.

0006-2960/94/0433-12247$04.50/0

site-directed fluorescence labeling of cysteine residues of the A-chain has been followed. Ricin A-chain contains two cysteine residues at positions 259 and 171 in the amino acid sequence. Cys 171 is buried inside an α-helix (Monfort et al., 1987; Katzin et al., 1991; Rutenber et al., 1991a,b) and is not easily accessible. Earlier experiments with the A-chain showed that the labeling by sulfhydryl reagents occurred mainly on Cys 259, which is involved in the interchain disulfide linkage (Ramakrishnan et al., 1989). I-AEDANS has been used (Lakey et al., 1993) as a reporter group for the membrane insertion experiments on colicin A. In a similar way the structural changes in the bound A-chain of ricin have been studied by energy transfer distance measurements between Trp 211 and AEDANS attached to Cys 259. Penetration depths of Cys 259 residue have also been measured by AEDANS fluorescence quenching with 5-, 10-, and 12-doxyl-PCs as well as 9,10-dibromo-PC using the parallax method of Chattopadhyay and London (1987).

MATERIALS AND METHODS

Materials

DOPC, DTT, HEPES, iodoacetamido-TEMPO, and I-AEDANS were obtained from Sigma Chemical Co. Spin-labeled PCs were procured from Avanti Polar Lipids. All column materials used for the protein purification were bought from Pharmacia. All other reagents were of spectroscopic grade and available locally. Purity of all lipids was checked on precoated silica gel TLC plates in a solvent of chloroform/methanol/water (65:35:5 v/v) and were developed using a phosphate sensitive spray. The concentration of phosphate in the spin-labeled PCs and DOPC was estimated according to the method of Fiske and Subba Rao (1925) and expressed in terms of total phosphate concentration. The spin concentration of all the spin-labeled lipids was estimated by doubly integrating the ESR spectral intensity of the lipids in an organic solvent and by comparison with an average of two known standards, TEMPO choline chloride and 4-hydroxy-TEMPO.

Brominated phospholipids were prepared by simple bromination of the double bond of the oleoyl group of DOPC (East & Lee, 1982). Briefly, 50 mg of DOPC in chloroform was added to 20 μL of bromine at −20 °C, and the reaction was allowed to proceed for 35 min. Excess bromine was removed by placing the reaction mixture on a silicic acid column preequilibrated with chloroform and eluting with 250 mL of chloroform first and with 250 mL of 10% (v/v) methanol in chloroform subsequently. Finally, the brominated phospholipid was eluted with 250 mL of 1:1 (v/v) chloroform/methanol. Fractions were collected, and TLC showed only one spot on precoated silica gel plates for the brominated phospholipid containing fractions. All such fractions were evaporated in a rotary evaporator. The evaporated phospholipid was then resuspended in chloroform/methanol (1:1 v/v) and stored under nitrogen at −20 °C. The number of bromines per phospholipid molecule was analyzed using the gold chloride method (Abrams et al., 1992). Dried phospholipids and sodium bromide standards containing 0.22–2.2 μmol of bromine were mixed with 200 μL of 5% potassium *tert*-butoxide in methanol, tightly kept in a screw-capped tube, and incubated for about 1 h at 110–120 °C. Subsequently, the samples were redried and 200 μL of methanol was added to each tube. Then 300 μL of 30% HNO_3, 100 μL of 3% Triton X-100, and 600 μL of methanol were added. The mixture was vortexed until it was clear, and 30 μL of gold chloride ($NaAuCl_4 \cdot 2H_2O$) was added (59 mg/10 mL) to each tube. After 10 min, the absorption was recorded at 440 nm. The bromine to phosphate ratio in 9,10-dibromo-PC was calculated to be 2.25 bromines per lipid (the expected value is 2). The purity was ascertained by TLC and mass spectrometry.

Protein Purification. Ricin and its constituent polypeptides were isolated as described in an earlier paper (Ramalingam et al., 1993). The purity of the proteins was checked by SDS–PAGE. All of the proteins showed single bands and were used without further purification.

AEDANS Labeling of the A-Chain. Ricin A-chain was reacted with a 5-fold excess of I-AEDANS in a dark room in HEPES buffer at pH 7.3 for 4 h. The excess unreacted label was removed by passing the sample through a Sephadex G-25 column at 4 °C. The labeled protein was dialyzed in the presence of DTT. The purity was checked by SDS–PAGE. The labeling efficiency was calculated from the extinction coefficient of I-AEDANS ($\epsilon_{340} = 6.0 \times 10^3\ M^{-1}\ cm^{-1}$) in solution (Lakey et al., 1991). Ricin A-chain was labeled at Cys 259 by iodoacetamido-TEMPO in a similar way to what was done for the AEDANS labeling. The extent of labeling was estimated using TEMPO choline chloride as the standard. The spin to protein ratio for the iodoacetamido-TEMPO-labeled A-chain was 0.89.

Liposome Preparation. A solution of 2.0 μmol of the synthetic phospholipid DOPC along with spin-labeled or brominated PC with or without GM_1 in chloroform was evaporated under nitrogen atmosphere in a glass vial to form a uniform film. The film was then desiccated under vacuum for 8–12 h, hydrated in 10 mM HEPES buffer containing 100 mM NaCl at pH 7.3 or in 10 mM acetate buffer at pH 4.5 containing the same amount of NaCl, and sonicated in a bath sonicator for about 20–25 min to near optical clarity. The resulting small unilamellar vesicles (SUV) were used in all experiments. GM_1 was maintained at 4 mol % in all liposomal preparations with the receptor.

Methods

Spectral Measurements. Fluorescence experiments were carried out at room temperature in a Shimadzu spectrofluorometer (RF-5000). For fluorescence quenching experiments, DOPC vesicles with different mole percentages of either spin-labeled or brominated phospholipids were used. The controls were lacking these spin-labeled and brominated PCs. However, for the experiments with receptor, DOPC/GM_1 vesicles were used as controls. Measurements were made with a 0.5-mL cuvette. For tryptophan quenching all experiments were done at an excitation wavelength of 295 nm. Care was taken to avoid inner filter effects by keeping the absorbance below 0.05. For AEDANS quenching fluorescence excitation was at 340 nm. For the A-chain insertion kinetics, the AEDANS emission was monitored at 480 nm after excitation at 380 nm. The excitation and emission bandwidths were kept at 5 nm in all experiments. All of the readings were taken 10 min after addition of liposomes.

For energy transfer measurements protein samples were dissolved in either 10 mM acetate buffer (pH 4.5) or HEPES (pH 7.3) containing 100 mM NaCl and 2 mM EDTA. The sample buffers were passed through Millipore filters to remove suspended particles prior to use. The quantum yields of the Trp 211 in the A-chain are taken as 0.27 and 0.25 at pH 7.3 and 4.5, respectively (Bushueva & Tonevitsky, 1987). The resonance energy transfer efficiency between Trp 211 donor and AEDANS acceptor was calculated (Gonzalez-Manas et al., 1992) from the fluorescence intensity of the Trp 211 in

the presence and absence of AEDANS by integrating all fluorescence intensities between 320 and 420 nm. The excitation wavelength was set at 295 nm. Any reduction in the fluorescence intensity was assigned to be due to energy transfer.

Tryptophan AEDANS Distance from Resonance Energy Transfer. Since the labeling efficiency was <100%, the transfer efficiency (E) is calculated as (Birks, 1970; Wang & Cheung, 1984; Lakey et al., 1993)

$$E = 1 - \frac{F_{DA} - F_D(1 - f_A)}{F_D f_A} \quad (1)$$

where F_D and F_{DA} represent the fluorescence of the donor, tryptophan, in the absence and in the presence of the acceptor, AEDANS, respectively, and f_A is the fractional occupancy of the acceptor sites. The measured efficiency was then used to calculate the donor–acceptor separation (R) as

$$R = (E^{-1} - 1)^{1/6} R_c \quad (2)$$

where R_c is the Forster distance at which E is 50% and is calculated in the usual manner as

$$R_c = (Jk^2 Q_0 n^{-4})^{1/6} (9.7 \times 10^3)\ \text{Å} \quad (3)$$

where n is the refractive index of the medium and is taken as 1.4, Q_0 is the quantum yield of the donor in the absence of the acceptor, k^2 is the orientation factor, and J is the overlap integral ($cm^3\ M^{-1}$). J is given by

$$J = \int F_D(\lambda)\epsilon_A(\lambda)\lambda^4 d\lambda / \int F_D(\lambda) d\lambda \quad (4)$$

where $F_D(\lambda)$ is the corrected fluorescence of the A-chain excited at 295 nm and $\epsilon_A(\lambda)$ is the extinction coefficient of the IAEDANS expressed in $M^{-1}\ cm^{-1}$. J was numerically integrated at 1-nm intervals and is found to be 2.38×10^{-15} $cm^3\ M^{-1}$. The orientation factor k^2 was taken as the isotropic value, $^2/_3$ (Birks, 1970).

ESR and CD Measurements. ESR spectra were recorded on a Varian E-9 spectrometer using glass capillaries. All spectra were measured using a microwave power of 2 mW with a modulation amplitude of 0.5 G except for the iodoacetamido-TEMPO-labeled A-chain, which was studied at 10-mW microwave power. The ratios of spin per molecule of DOPC were 0.80, 0.88, and 0.85 for 5, 10, and 12 spin-labeled PCs, respectively.

CD measurements were made in a Jasco (J-500A) spectropolarimeter. Samples were scanned four times at the rate of 20 nm/min and averaged. The temperature of the sample compartment was maintained with a circulating water bath. A blank run was made with the liposomes alone and subtracted from the experimental spectra. All spectra were smoothed and converted to the mean residue ellipticity, θ in deg cm^2 $dmol^{-1}$, using mean residue molecular weights of 110 for the A-chain, 109 for the B-chain, and 109.6 for intact ricin (Frenoy, 1986; Wawrzynczak et al., 1988). Calculations of the fractional percentage of α-helix were done by measuring the change in the ellipticity value at 222 nm. The α-helix content was calculated as (Wu et al., 1981)

$$f_h = (\theta_{222} - \theta^0{}_{222})/\theta^{100}{}_{222} \quad (5)$$

where θ_{222} is the experimentally measured mean residue ellipticity at 222 nm. $\theta^{100}{}_{222}$ and $\theta^0{}_{222}$ correspond to 100% and 0% helix content, estimated as −30 000 and 2000 deg cm^2 $dmol^{-1}$, respectively (Gazit & Shai, 1993).

Quenching Measurements. The fluorophore depth was obtained from the expression (Chattopadhyay & London, 1987)

$$z_{cF} = L_{c1} + \{[(-1/\pi C)\ln(F_1/F_2) - L_{21}{}^2]/2L_{21}\} \quad (6)$$

where z_{cF} is the distance of the fluorophore from the center of the bilayer, L_{c1} is the distance of the shallow quencher measured from the bilayer center, and L_{21} is the difference in depth between two spin labels. C is the concentration of the quencher per unit area, and F_1/F_2 is the ratio of F_1/F_0 and F_2/F_0 in which F_1 and F_2 are fluorescence intensities of two sets of samples with quenchers 1 and 2, respectively, at the same quencher concentration, C. F_0 is the fluorescence intensity in the absence of a quencher. This quantitative estimation is possible due to the ability of both brominated and spin-labeled phospholipids to quench the intrinsic Trp fluorescence of the proteins (Abrams et al., 1992) over a short range.

RESULTS

Figure 1a shows the tryptophan fluorescence quenching of the ricin B-chain by addition of SUVs containing one of the three spin-labeled PCs and DOPC without the receptor, GM_1, at pH 4.5. The B-chain is more efficiently quenched by 5-doxyl-PC. Similar observations were made with SUVs containing 9,10-dibrominated PC and DOPC (data not shown). In sharp contrast to the B-chain, the A-chain shows stronger quenching with 10- or 12-doxyl spin labels (see Figure 1b). This is further confirmed by quenching studies with dibrominated PCs (data not shown). For the A- and B-chains the extent of quenching is less at pH 7.3 than at pH 4.5. Quenching by brominated PC is comparable with that of the 10-doxyl-PC under similar conditions. In the presence of GM_1 (4 mol %), intact ricin shows a stronger quenching in the tryptophan fluorescence with 5-doxyl-PC than with 10- or 12-doxyl-PC or dibrominated PCs (Figure 1c), but for vesicles without GM_1, the decrease in fluorescence is not significant at pH 7.3. In other words, a receptor seems necessary for the protein to interact with the membrane at pH 7.3. However, at pH 4.5 (Figure 1d) quenching of tryptophan fluorescence in intact ricin takes place with SUVs of spin-labeled PC and DOPC without GM_1 and the quenching is ~45% at 0.7 mol % of 5-doxyl-labeled lipid (at lipid:protein = 22). The calculated penetration depths are listed in Table 1. Since both ricin and its B-subunit have multiple tryptophan residues, the observed intensity is actually the sum over the fluorescence of each tryptophan weighed by its quantum yield and the observed depth is, thus, an average value over all tryptophan distances from the quencher. To the contrary, the A-chain has a single tryptophan at position 211 and the calculated depth reflects its exact location in the membrane. The average penetration depths for ricin and its B-chain are comparable and are approximately 11 and 13 Å from the center of the bilayer at pH 4.5 and 7.3, respectively. The A-chain, on the other hand, shows a penetration depth of 9 Å at neutral pH. The intrusion into the bilayer is deeper and the Trp 211 is located 8 Å away from the bilayer center at pH 4.5. Figure 2 shows the pH-dependent change in the F/F_0 value of the intrinsic aromatic fluorescence of intact ricin and its A-chain (parts a and b, respectively) by SUVs containing one of the

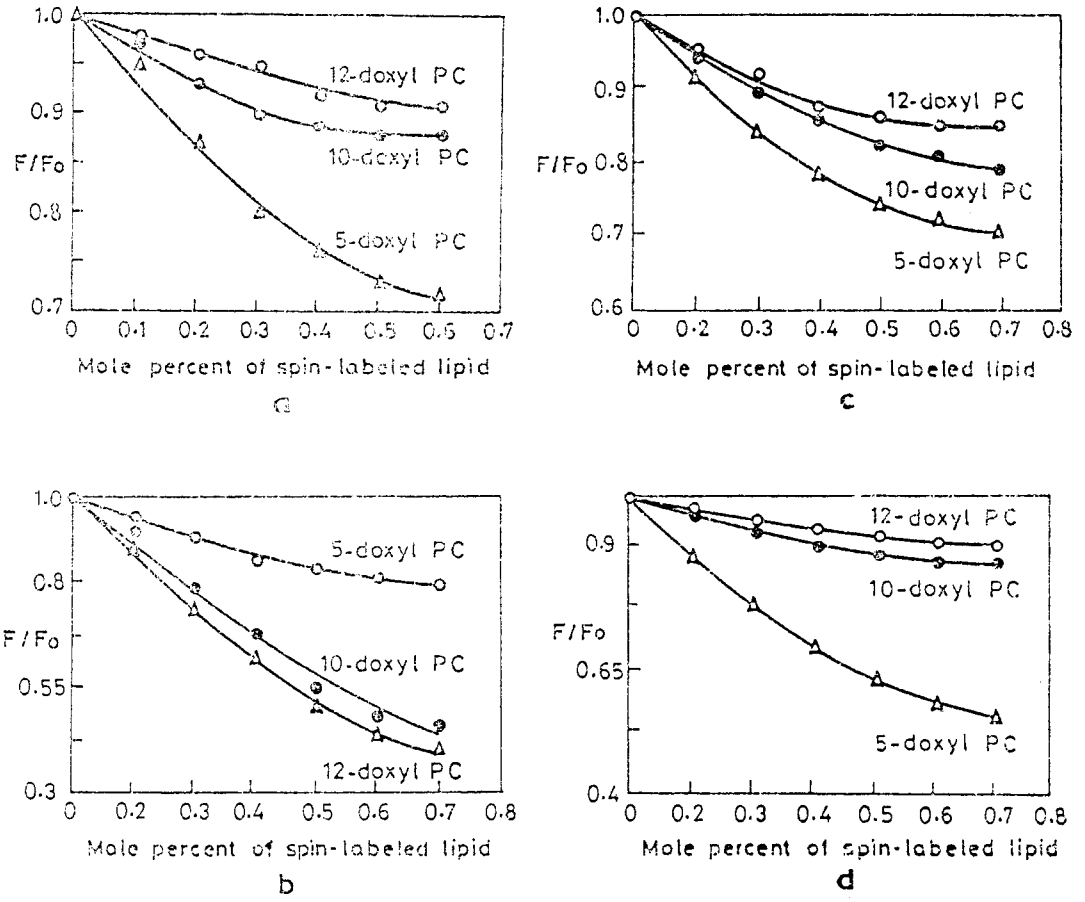

FIGURE 1: Quenching of Trp fluorescence of the protein added to aqueous small unilamellar vesicles containing one of the three spin-labeled PCs and DOPC at different pH values. The abscissa is the mole percent of the spin-labeled lipid in the lipid mixture. The ordinate is the ratio of the fluorescence in the presence (F) and absence (F_o) of the spin-labeled lipid. (a) Ricin B-chain in acetate buffer (pH 4.5): the concentrations of the protein and lipid are 1.5 and 25 μM (total lipid), respectively. (b) Ricin A-chain in acetate buffer (pH 4.5): the concentrations employed were 2 μM A-chain and 27 μM total lipid. (c) Intact ricin was added to small unilamellar vesicles containing one of the three spin-labeled PCs, DOPC, and GM_1 (4 mol %) in HEPES buffer (pH 7.3). Protein concentration was 1.4 μM and lipid concentration, 30 μM. (d) Intact ricin in acetate buffer (pH 4.5): concentrations of ricin and total lipid are 1.4 and 30 μM, respectively.

Table 1: Penetration Depths of Tryptophan(s)

protein	pH	spin-labeled PC pair used for quenching analysis	distance calculated from the center of the bilayer (Å)	Z_{av} (Å)
ricin	7.3	5–10	12.5	12.9
		5–12	13.2	
	4.5	5–10	10.7	10.0
		5–12	9.2	
A-chain	7.3	5–10	10.0	9.0
		5–12	8.0	
	4.5	5–10	8.0	7.6
		5–12	7.2	
B-chain	7.3	5–10	13.5	12.7
		5–12	12.0	
	4.5	5–10	13.0	12.5
		5–12	12.0	

three doxyl-PCs and DOPC. A transition in the extent of quenching occurred at pH 5.5 for intact ricin as well as the A-chain. This inflection point is coincident with the change of conformation of the native protein as reported by Frenoy (1986) from the effect of pH on the ricin CD spectrum. Therefore, a change in folding of the A-chain as well as intact ricin at pH ~5.5 in the solution may facilitate toxin insertion into the membrane bilayer.

Figure 3 displays the fluorescence spectra of AEDANS-labeled A-chain in the presence and absence of DOPC SUVs at pH 7.3. The fluorescence spectra exhibit a maximum around 480 nm which shifts to the blue by ~10 nm in the presence of the vesicles accompanied by a huge increase in the fluorescence intensity. Acrylamide did not quench the protein–AEDANS fluorescence at either pH (data not shown), indicating that the AEDANS-labeled Cys 259 was situated deep inside the bilayer. To confirm this in another way, we employed 5-, 10-, and 12-doxyl-PCs and 9,10-dibrominated PC as quenchers of the AEDANS fluorescence of the labeled A-chain using the parallax method (Chattopadhyay & London, 1987). The depth-dependent quenching measurements show that 10- and 12-doxyl-PC and brominated PCs are able to quench the fluorescence more efficiently than the 5-doxyl-PC. The apparent depths calculated by eq 6 are listed in Table 2. These data indicate that AEDANS is located deep in the bilayer interior and is about ~10 Å from the center. The Trp 211 depth was also estimated in the AEDANS-labeled A-chain and is comparable to the value obtained for the unlabeled protein.

Insertion Kinetics of the A-Chain. The kinetics of membrane insertion at acidic and neutral pH was monitored by measuring the fluorescence intensity of AEDANS of the Cys

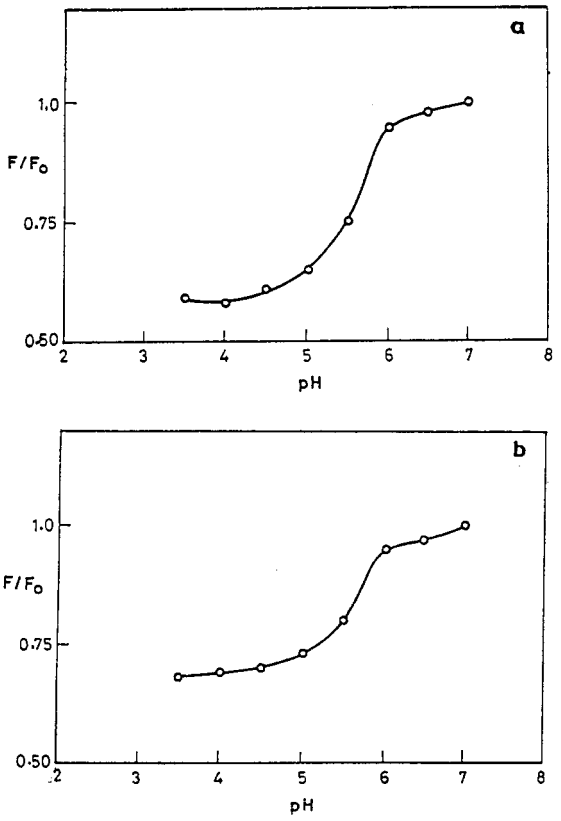

FIGURE 2: Effect of pH on ricin binding to the DOPC membrane monitored by quenching by nitroxide spin labels. (a) Quenching of intrinsic aromatic fluorescence of intact ricin by membrane-bound 5-doxyl-PC. Ricin (3.0 μM) in HEPES buffer was titrated with HCl in the presence of small unilamellar vesicles containing 5-doxyl-PC, DOPC, and GM_1 (4 mol %). The total lipid concentration was 35 μM. The ratio of DOPC to spin-labeled PC is 0.005 (mole/mole). (b) Quenching of the aromatic fluorescence of the toxic A-chain by membrane-bound 10-doxyl-PC. The ratio of DOPC to spin-labeled PC is 0.005 (mole/mole); 2.0 μM A-chain was employed with 35 μM total lipid.

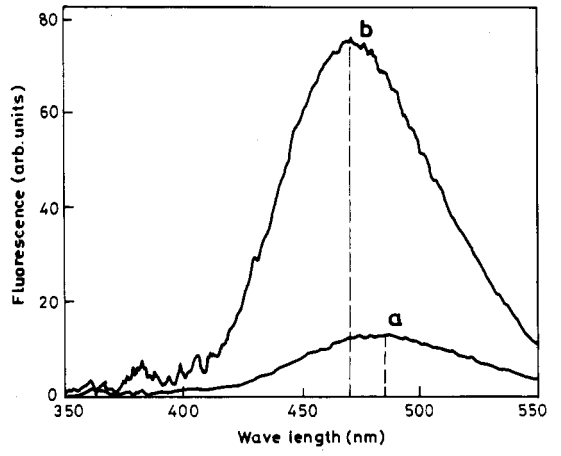

FIGURE 3: Fluorescence spectra of AEDANS-labeled ricin A-chain in the absence (a) and presence (b) of liposomes at pH 7.3. Concentrations of the A-chain and lipid are 2.0 and 40.0 μM (total lipid), respectively. Excitation was at 340 nm.

259 labeled protein at 480 nm after addition of DOPC SUVs as a function of time, and the results are displayed in Figure 4. At initial time $t = 0$ all of the protein is free and the fluorescence is F_0; at infinite time ($t \rightarrow \infty$) the insertion is complete and $F = F_\infty$. At any time t, the intensity is $F(t)$ and the rate constant, k, for the A-chain insertion to the membrane was obtained by plotting $\ln[(F_t - F_\infty)/(F_0 - F_\infty)]$ vs time. This plot gives a straight line, showing that the primary insertion process into the membrane is monophasic. The insertion process is over in ca. 3 min, indicating that the penetration of the membrane by the A-chain is a single-step process. Also, the rate of insertion of the ricin A-chain is higher at acidic pH ($k = 1.95 \times 10^{-2}$ s^{-1}) than at neutral pH ($k = 1.06 \times 10^{-2}$ s^{-1}). A similar behavior has been observed for insertion of colicin A into small Br–DOPG vesicles (van der Goot et al., 1991).

Resonance Energy Transfer between Tryptophan and AEDANS. We exploited the energy transfer between two unique fluorophores in the labeled A-chain, namely the intrinsic Trp 211 and chemically attached AEDANS at Cys 259, to estimate their relative position in the membrane. Figure 5 shows the aromatic fluorescence of the A-chain excited at 295 nm in the absence as well as presence of the AEDANS chromophore. The extent of energy transfer is 74% in the absence of the membrane at neutral pH. This is not significantly affected by the pH of the medium as seen from Table 3. The transfer efficiency is greatly reduced from 74% and 72% to 50% and 25% at neutral and acidic pH, respectively, in the presence of the membrane. The estimated distances from the energy transfer data reveal that there is a larger separation between Trp 211 and Cys 259 in the membrane-embedded state than in the solution. The AEDANS excitation spectrum of the labeled A-chain using the emission maximum at 480 nm was also measured (data not shown). An observed increase in the band intensity between 290 and 300 nm indicated that energy transfer from Trp 211 is, indeed, taking place.

Effect of SUVs on the Protein CD Spectra. Figure 6a displays the CD spectra (200–250 nm) of the ricin A-chain. It shows the presence of both α-helix and β-strand structures. Addition of DOPC SUVs changes the α-helix content judged by the change in the mean residue ellipticity at 222 nm. At both pH 4.5 and 7.3 the helical content of the protein increases after addition of DOPC liposomes (protein:lipid ratio = 1:15). This shows that the A-chain binding to the membrane is accompanied by a change in the secondary structure of the protein. Ricin also shows similar behavior after interacting with DOPC liposomes. Figure 6b shows the CD spectra of ricin. The helix content increases by 8% on binding to the membrane at pH 7.3. At acidic pH a greater increase (12%) in the helical content is observed. The presence of GM_1 in DOPC vesicles altered the spectrum only marginally ($\leq$2%) at either pH. The α-helical content of both ricin and its A-chain on binding to liposomes is plotted in Figure 7 as a function of pH. It appears that the helical content increases suddenly for both proteins in going from pH 6 to 5, with the midpoint of transition at pH 5.5. Therefore, at pH <5.0, the protein membrane interaction is favorable and the secondary structure of the protein alters to gain maximum stabilization inside the membrane. The CD spectrum of the ricin B-chain has a broad negative band at 200–225 nm with a small positive peak at 230 nm (spectrum not shown) with far less overall ellipticity compared to the native protein. Therefore, the B-chain spectra were not analyzed for change in the secondary structure.

DISCUSSION

Fluorescence quenching results demonstrate that binding of lipid vesicles to intact ricin and its B-chain is mainly receptor mediated at neutral pH. It is also observed that the B-chain associates with the membrane on its own at neutral pH as evidenced by ~25% quenching of tryptophan fluorescence by spin-labeled PCs. The quenching is more efficient with

Table 2: Calculated Penetration Depths of AEDANS and Tryptophan(s) in AEDANS-Labeled A-Chain

fluorophore of labeled A-chain used in depth calculation	pH	spin-label pair used in penetration depth determination	distance calculated from the center of the bilayer (Å)	Z_{av} (Å)
AEDANS	7.3	5–10	11.0	10.5
		5–12	10.0	
	4.5	5–10	10.1	9.5
		5–12	8.9	
Trp 211	7.3	5–10	10.1	9.8 (9.0)[a]
		5–12	9.4	
	4.5	5–10	8.6	8.3 (7.6)[a]
		5–12	8.0	

[a] Values calculated for the unlabeled A-chain.

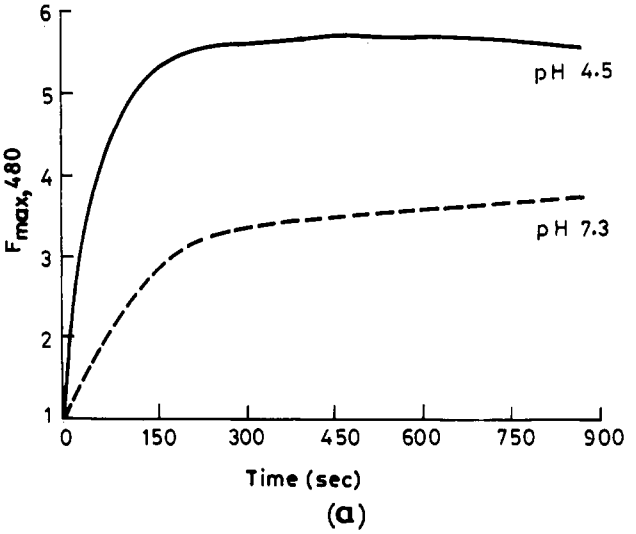

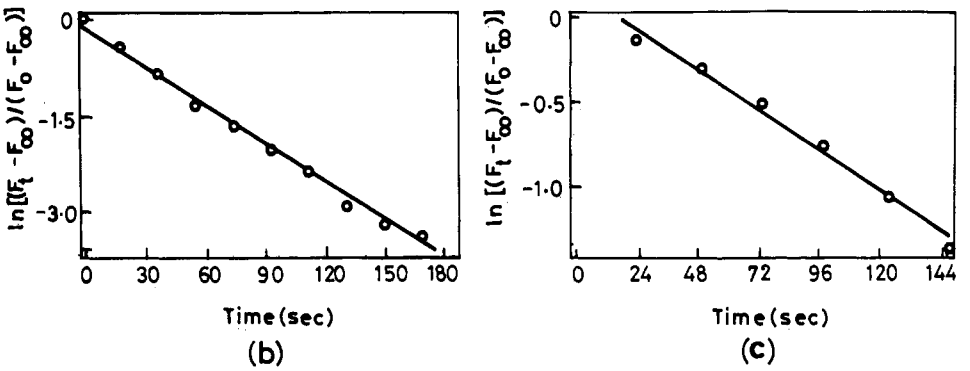

FIGURE 4: (a) Kinetics of AEDANS-labeled ricin A-chain insertion into the DOPC membrane monitored by fluorescence changes at 480 nm. The excitation wavelength was set at 380 nm. (b and c) Plots of $\ln(F_t - F_\infty/F_0 - F_\infty)$ vs time at pH 4.5 and 7.3, respectively. The slope of the plot is $-k$ ($k = 1.95 \times 10^{-2}$ s^{-1} at pH 4.5; $k = 1.06 \times 10^{-2}$ s^{-1} at pH 7.3). AEDANS-labeled A-chain (0.9 μM) was employed in the experiments.

5-doxyl-PC than with 10- or 12-doxyl-PCs, suggesting that both proteins are located close to the interfacial region. This is apparent from the measured penetration depths. The A-chain, on the contrary, penetrates deep into the membrane at pH 7.3 as well as at acidic pH (4.5). The penetration depth of AEDANS attached to Cys 259 is ~10 Å. Both Trp 211 and Cys 259 are at the two extremes of domain 3 of the A-chain structure (Katzin et al., 1991). A closer look at domain 3, made up of amino acid residues 211–267, reveals that there is a long hydrophobic stretch near the C terminus: residues 247–257 are Ile-Leu-Ile-Pro-Ile-Ile-Ala-Leu-Met-Val. Since we observe a deep penetration or substantial quenching of both Trp 211 and AEDANS, it is likely that this domain of the protein is well inside the membrane. The more hydrophobic character of ricin and its A-chain at pH 4.5 compared to the native state (Ramalingam et al., 1993; Houston, 1982) may expose the hydrophobic stretch of residues 247–257 and thus facilitate membrane insertion. Increased hydrophobicity

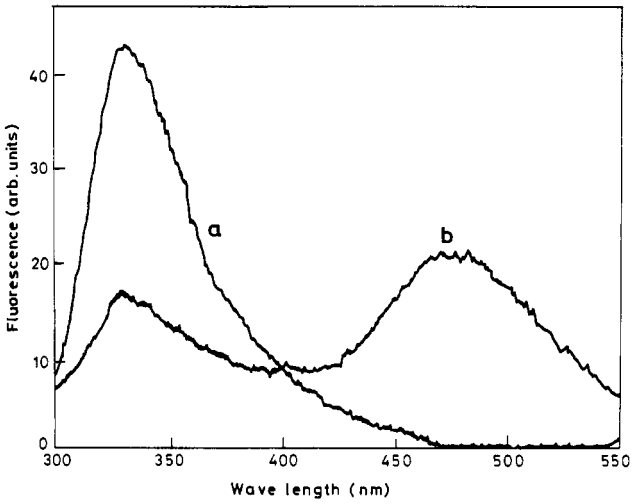

FIGURE 5: Energy transfer measurements: (a) fluorescence of the unlabeled A-chain (1.2 μM) at pH 7.3 by exciting at 295 nm; (b) fluorescence of the AEDANS-labeled A-chain at the above conditions.

Table 3: Donor–Acceptor Distances Measured from Energy Transfer in the AEDANS-Labeled A-Chain

AEDANS-labeled A-chain	pH	E (%)	R (Å)
–DOPC	7.3	74	16.6
+DOPC		50	19.8
–DOPC	4.5	72	16.9
+DOPC		25	23.7

relative to the native state is a characteristic property of a "molten globule" state (Kuwajima, 1989), and at pH 5.5 we probably see this structural transition. The partially unfolded conformation is then stabilized inside the membrane by hydrophobic contacts.

The distance calculated from the energy transfer data shows that the Trp 211 and AEDANS are separated by ~16.5 Å in solution, which is close to the distance between Trp 211 and Cys 259 (~15 Å) in the A-chain, calculated from the crystal coordinates available from the Cambridge Protein Databank. This implies similar packing arrangements in the solution and crystalline forms. In the presence of the membrane there is a significant increase (~7.0 Å at pH 4.5) in the separation between them (see Table 3). This can be explained in the following manner. The C-terminal end of the A-chain is mostly random coil, and on membrane binding, the folding pattern changes drastically, forcing Trp 211 to move away from Cys 259 laterally (since the penetration depths of these two chromophores measured from the bilayer center are similar). This is also accompanied by an increase in the overall helical structure of the protein as seen from the CD spectra. In other words, there is a structural requirement for the proteins to insert into the membrane. The cleavage of the disulfide bond connecting the A- and B-chains exposes the hydrophobic parts of the A-chain, which is stabilized at low pH by protonation of certain amino acid residues such as Glu, Asn, and His (Ramalingam et al., 1993). These domains are further stabilized by interaction with the membrane, and in the process the proteins undergo partial unfolding.

CONCLUSION

In cellular systems it seems likely that the B-chain of intact ricin binds to a surface receptor having a terminal galactose moiety and undergoes endocytosis. Subsequently, the intact ricin escapes from the endocytotic vesicles into the cytosol. However, the penetration of the B-chain into the membrane, even in the absence of receptors as demonstrated in the present work, suggests an alternate possibility of a translocating domain within the B-chain which facilitates the transfer of intact ricin into the cytosol. Therefore, unlike diphteria toxin B-chain, which is rich with hydrophobic residues, the B-chain in ricin participates in the translocation process. The rupture of the disulfide bond is necessary to liberate the A-chain to exhibit toxicity. We have also observed that the free A-chain is capable of translocating itself and that its C-terminal end is definitely involved in the first step of the translocation process. The initial penetration follows first-order kinetics. However, we are not sure if the rest of the protein is inside the bilayer or if a large part of the protein is protruding into the water-soluble part. Enzymatic cleavage experiments are underway in our laboratory to ascertain this.

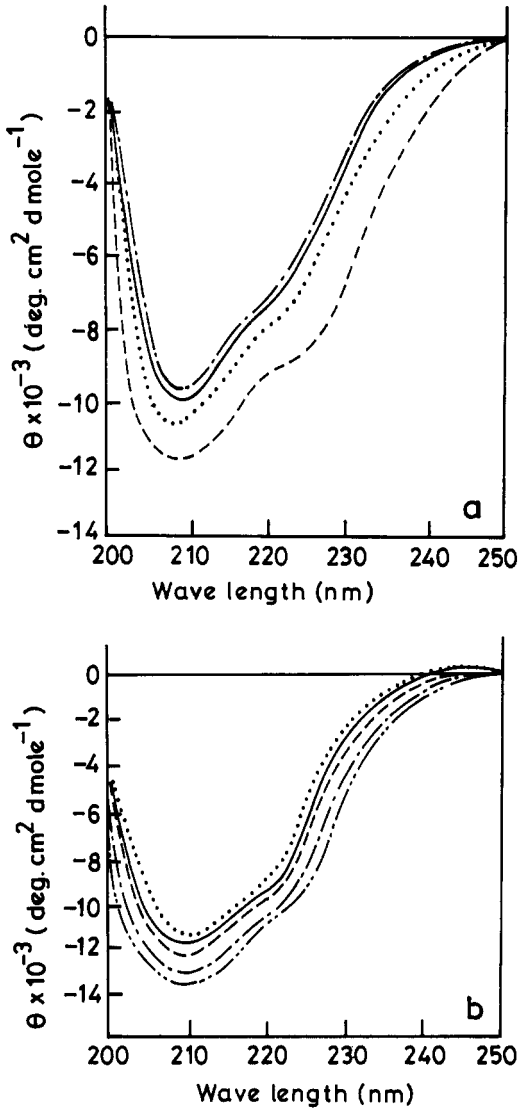

FIGURE 6: (a) Effect of SUVs on the far-UV CD spectra of the ricin A-chain: 7 μM A-chain in 10 mM HEPES buffer (pH 7.3) (dot-dash line); 7 μM A-chain in the presence of DOPC vesicles at pH 7.3 (dotted line); 6.7 μM A-chain in 10 mM acetate buffer (pH 4.5) (solid line); 6.7 μM A-chain at pH 4.5 plus DOPC liposomes (broken line). (b) Effect of SUVs on the CD spectra of intact ricin: 4.0 μM ricin in 10 mM HEPES buffer (dotted line); 4.0 μM ricin at pH 7.3 + 60 μM DOPC/GM_1 vesicles (solid line); 4.1 μM ricin in 10 mM acetate buffer (broken line); 4.1 μM ricin at pH 4.5 in the presence of DOPC vesicles (dot-dash line); 4.1 μM ricin at pH 4.5 with DOPC/GM_1 vesicles (dot-dot-dash line).

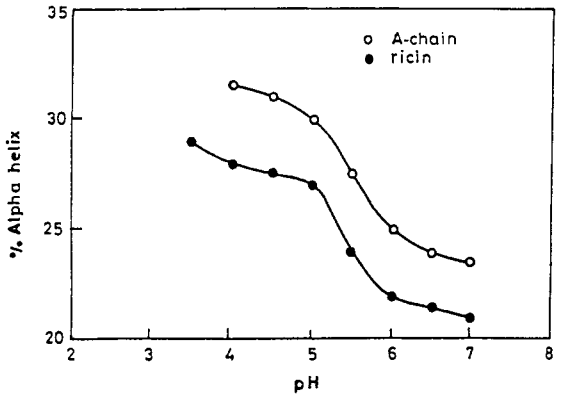

FIGURE 7: Percent α-helix of ricin and its A-chain in the presence of DOPC liposomes as a function of pH. DOPC (100 μM) and 10 μM ricin or 8.7 μM A-chain in 10 mM buffer were used. pH of the solution was decreased gradually by adding small aliquots of 4 N HCl into the buffer medium. Percentage α-helicity was calculated as described in the text.

ACKNOWLEDGMENT

We are grateful to Prof. K. R. K. Easwaran for allowing us to use the CD spectrometer. We thank Profs. P. Balaram and V. Raghavan for enlightening discussions. We also thank Prof. M. Edidin for critical reading of the manuscript.

REFERENCES

Abrams, F. S., Chattophadhyay, A., & London, E. (1992) *Biochemistry 31*, 5322–5327.
Beaumelle, B., Bensammar, L., & Bienvenue, A. (1992) *J. Biol. Chem. 267*, 11525–11531.
Beaumelle, B., Alami, M., & Hopkins, C. R. (1993) *J. Biol. Chem. 268*, 236661–23669.
Birks, J. B. (1970) *Photophysics of Aromatic Molecules*, pp 341–347, Wiley-Interscience, London.
Blatter, W. A., Lambert, J. M., & Goldmacher, V. S. (1989) *Cancer Cells 1*, 50–55.
Bushueva, T. L., & Tonevitsky, A. G. (1987) *FEBS Lett. 215*, 155–159.
Calafat, J., Molthoff, C., Janssen, J., & Hilkens, J. (1988) *Cancer Res. 48*, 3822–3827.
Chattophadhyay, A., & London, E. (1987) *Biochemistry 26*, 39–45.
Chattopadhyay, A., & McNamee, M. G. (1991) *Biochemistry 30*, 7159–7164.
Donovan, J. J., Simon, M. I., & Montal, M. (1985) *J. Biol. Chem. 260*, 8817–8823.
East, J. M., & Lee, A. G. (1982) *Biochemistry 21*, 4144–4151.
Fiske, C. A., & Subba Rao, Y. (1925) *J. Biol. Chem. 66*, 675–678.
Frenoy, J.-P. (1986) *Biochem. J. 240*, 221–226.
Frenoy, J.-P., Turpin, E., Janicot, M., Gehin-Fouque, F., & Desbouquois, B. (1992) *Biochem. J. 284*, 249–257.
Gazit, E., & Shai, Y. (1993) *Biochemistry 32*, 3429–3436.
Gill, D. M., Hope, J. A., Meren, R., & Jacobs, D. S. (1981) in *Receptor-mediated Binding & Internalisation of Toxins & Hormones* (Middlebrook, J. C., & Kohn, L. D., Eds.) pp 113–121, Academic, New York.
Gonzalez-Manas, J. M., Lakey, J. H., & Pattus, F. (1992) *Biochemistry 31*, 7294–7300.
Houston, L. L. (1982) *J. Biol. Chem. 257*, 1532–1539.
Hu, V. W., & Holmes, R. K. (1984) *J. Biol. Chem. 259*, 12226–12233.
Jiang, J. X., Abrams, F. S., & London, E. (1991) *Biochemistry 30*, 3857–3864.
Katzin, B. J., Collins, E. J., & Robertus, J. D. (1991) *Proteins: Struct., Funct. Genet. 10*, 251–259.
Kuwajima, K. (1989) *Proteins: Struct., Funct. Genet. 6*, 87–103.
Lakey, J. H., Baty, D., & Pattus, F. (1991) *J. Mol. Biol. 218*, 639–653.
Lakey, J. H., Duche, D., Gonzalez-Manas, J.-M., Baty, D., & Pattus, F. (1993) *J. Mol. Biol. 230*, 1055–1067.
London, E. (1992) *Biochim. Biophys. Acta 1113*, 25–51.
Markello, T., Zlotnick, A., Verett, J., Tennyson, J., & Holloway, P. W. (1985) *Biochemistry 24*, 2895–2901.
Monfort, W., Villafranca, J. E., Monzingo, A. F., Earnst, S., Katzin, B., Rutenber, E., Xuong, N. H., Hamlin, R., Robertus, J. D. (1987) *J. Biol. Chem. 262*, 5398–5403.
Montesano, D., Cawley, D., & Herschman, H. R. (1982) *Biochem. Biophys. Res. Commun. 109*, 7–13.
Olsnes, S., & Pihl, A. (1980) in *Molecular Actions of Toxins and Viruses* (Cohen, P., & van Heyningen, S., Eds.) pp 51–106, Elsevier, New York.
Olsnes, S., Moskaug, J., Stenmark, H., & Sandvig, K. (1988) *Trends Biochem. Sci. 13*, 348–351.
Ramakrishnan, S., Bjorn, M. J., & Houston, L. L. (1989) *Cancer Res. 49*, 613–617.
Ramalingam, T. S., Das, P. K., & Podder, S. K. (1993) *Biopolymers 21*, 1687–1694.
Rutenber, E., & Robertus, J. D. (1991a) *Proteins: Struct., Funct. Genet. 10*, 260–269.
Rutenber, E., Katzin, B. J., Ernst, S., Collins, E. J., Mlsna, D., Ready, M. P., & Robertus, J. D. (1991b) *Proteins: Struct., Funct. Genet. 10*, 240–250.
Sekharam, K. M., Badrick, T., & Georgnion, S. (1991) *Biochim. Biophys. Acta 1063*, 171–174.
Utsumi, T., Aizono, Y., & Funatsu, G. (1984) *Biochim. Biophys. Acta 772*, 202–208.
Utsumi, T., Aizono, Y., & Funatsu, G. (1987) *FEBS Lett. 216*, 99–103.
van der Goot, F. G., Gonzalez-Manas, J. M., Lakey, J. H., & Pattus, F. (1991) *Nature 354*, 408–410.
Vietta, E. S., & Thorpe, P. E. (1993) *Immunol. Today 14*, 252–259.
Wang, C.-K., & Cheung, H. C. (1984) *J. Mol. Biol. 190*, 509–521.
Wawrzynczak, E. J., Drake, A. F., & Thorpe, P. E. (1988) *Biophys. Chem. 31*, 301–305.
Wu, C. S. C., Ikeda, K., & Yang, J. T. (1981) *Biochemistry 20*, 566–570.